Loop impedance measurement tool

Johan Abrahamsson

2020-08-28

LiU LINKÖPINGS UNIVERSITET

Department of Science and Technology
Linköping University
SE-601 74 Norrköping, Sweden

Institutionen för teknik och naturvetenskap
Linköpings universitet
601 74 Norrköping

Loop impedance measurement tool

The thesis work carried out in Elektroteknik
at Tekniska högskolan at
Linköpings universitet

Johan Abrahamsson

Norrköping 2020-08-28

LiU LINKÖPINGS UNIVERSITET

Department of Science and Technology
Linköping University
SE-601 74 Norrköping, Sweden

Institutionen för teknik och naturvetenskap
Linköpings universitet
601 74 Norrköping

Abstract

This master's thesis presents a prototype of a hand-held measurement tool used to measure the loop impedance of ground loops using two current probes. This tool allows the user to find bad shield connections in a system without disconnecting the shielded cables. The thesis explains the theory behind the measurement method, hardware requirements and design, how the software works and a demonstration of the implemented graphical user interface. The tool is powered by a two-cell lithium-ion battery and has an integrated battery charger with cell balancing.

Acknowledgments

I would like to thank Linköpings University for the education that made this master's thesis possible. At the university I would like to give and extra thank to my examiner Qin Zhong-Ye and my supervisor Amir Baranzahi for the advice and support I have gotten throughout the project. I am grateful to Saab Dynamics AB for allowing me this opportunity and the embrace received by all their employees. Special thanks to Clas Tegenfeldt, my supervisor at Saab Dynamics, whom came with much good information and explanations about the subject of this master's thesis project. I would also like to thank my boss at Saab Dynamics, Mattias Karlsson, for being very supportive during the whole project and for the help with all the administrative problems.

Contents

List of Figures

viii

List of Tables

List of Acronyms

AC Alternating Current

ADC Analog to Digital Converter

BMS Battery Management System

DAC Digital to Analog Converter

DC Direct Current

DMA Direct Memmory Access

DUT Device Under Test

EMC Electromagnetic Compatibility

FPGA Field-Programmable Gate Array

I2C Inter-Integrated Circuit

IDE Integrated Development Environment

MCU Microcontroller Unit

MOSFET Metal Oxide Semiconductor Field Effect Transistor

PCB Printed Circuit Board

PWM Pulse Width Modulation

SE Shielding Effectiveness
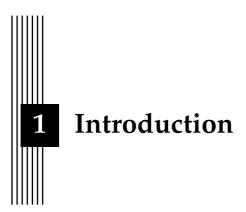
SoC System on a Chip

SPI Serial Peripheral Interface

SSR Solid-State Relay

USB Universal Serial Bus

Zt Transfer Impedance

1 Introduction

This master's thesis designs and develops a measurement tool to measure shield impedance of cables within a system. This project was done as a master's thesis at the Electronic Design Engineering program at Linköpings University provided by Saab Dynamics in Linköping, Sweden.

1.1 Background

Saab Dynamics develops state-of-the-art electronics in safety-critical applications. This electronics need to work in the most extreme environments of cold, heat, vibration, interference and radiation. It should work flawlessly from the first second - even after 25 years. Everywhere, electronics are used which are becoming more advanced, compact, energy efficient and work with ever higher frequencies. We use more and more wireless technology for good and evil. Society's growing dependence on electrical systems and communication systems today demands more and more that no one else interferes or is disturbed, that is what we call EMC.

EMC stands for electromagnetic compatibility. The electromagnetic spectrum is a limited common resource. Therefore, different systems must be designed to work without interfering with each other. There are legal, commercial, technical, military, practical and theoretical aspects within EMC. Important parts of EMC are design, measurement technology, testing and verification.

The electric fields, magnetic fields or radio frequency radiation that a product is in, is something we call the electrical environment. A mobile phone sends a radiation utility signal to communicate with the base station, but can at the same time interfere with radios and other electronics. In principle everything can be seen as a disturbance of the electrical environment. Disturbances can go wireless as an electromagnetic wave in space or follow wires, and an apparatus can interfere or be disturbed. In short, we have transmitter-channel-receivers and the EMC work tries to handle all three parts.

A classic way is to try to shield themselves from the environment through dense metal boxes and use shielded cables between them. But what will happen if the cable is not connected properly? How can one detect a leak of interference caused by a cable and its connectors in existing systems currently in use?

1.2 Aim

The aim of this master's thesis work is to develop a practical method to measure how good a shielded cable is, where the connected equipment is in a complex system, even though the cable connector has been unscrewed and remounted many times. The method should then be realized by designing a portable measurement tool that easily can be used to measure the condition of a shielded cable without disconnecting it.

1.3 Research questions

The main questions of this project are presented here and will be answered later in this report.

1. How can the loop impedance reveal the condition of a shielded cable?

2. How can a specific connector be examined to see if it has been oxidized without removing the connector?

3. How can a filter be designed to allow programmable center frequency?

2 Shield Impedance Measurement Techniques and Implementation Requirements

2.1 Shielding Effectiveness

Shielding effectiveness is a dimensionless number, which describes how good a shield isolates the leakage of radiated emissions.[3] For any shielding barrier, shielding effectiveness (SE) is given by:

$$SE(dB) = 20log\frac{[E \ (\ or \ H) \ without \ shield]}{[E \ (or \ H) \ with \ shield]} \tag{2.1}$$

By exposing a test cable of a strong known electromagnetic field, the shielding effectiveness can be calculated by measuring the electromagnetic field inside the cable between the shield and the core. In practice, this electromagnetic field is very hard to measure since it is confined between the shield and the core and hard to access with a measurement tool. Instead the voltage between shield and core can be measured while illuminating a strong electromagnetic field, but this method requires expensive measurement equipment and gives much room for measurement errors.[4]

2.2 Transfer Impedance

Another way of measuring the condition of the shield is by measuring the transfer impedance (Z_t) for the cable shield. In contrast to measure the shielding effectiveness, this is a purely conducted measurement method with accurate results. But Z_t has the dimension Ω/m and cannot be directly seen as the shield performance. It can however be used to calculate the shield performance [8]. The problem with this method is that it requires disassembly of the system to measure allow measurement of the transfer impedance of a specific shielded cable [11].

2.3 Loop Resistance

By measuring a total resistance of a loop, a bad connector or a break can be found. Since a bad connector gives a higher resistance, there will be a relatively large potential over the connector. This potential can be measured to find where the bad connection is. This voltage measurement is required to determine if the total loop resistance is high because of a specific connector or if the conductivity in the whole loop is low.[6]
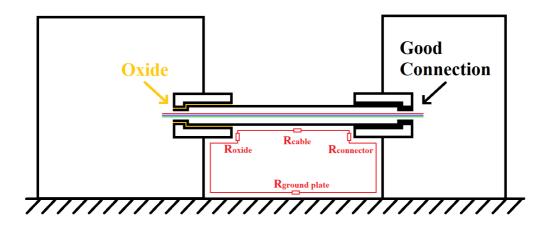
Figure 2.1: Two shielded boxes connected to the same ground plane, connected with a shielded cable and connectors.

The loop resistance can be measured using two probes. One injecting probe which injects a strong signal with a low frequency. The signal is then measured using a measurement probe. If the losses at the specific frequency is known for the two probes, the loop resistance can be calculated. This is explained in detail in section 3.1 Measure Impedance.

This method is good enough since the total max impedance of the shield is specified for most military products, and it gives a good first result to know if the shield performance need to be evaluated more in detail with more accurate methods.

2.4 Current Probe Injection

A current probe woks similar to a transformer with only one winding on one of the two sides. Figure 2.2 show an ideal current probe. When a current I flows through the conductor, magnetic flux B is generated in the core. This magnetic flux induces a current in the second wire which is proportional to the current I.[1]

The magnetic flow in a coil with N turns can be explained with the formula $N\Phi = BA$ where Φ is the magnetic flow through one turn, B is the magnetic flux and A is the cross section area of the coil.
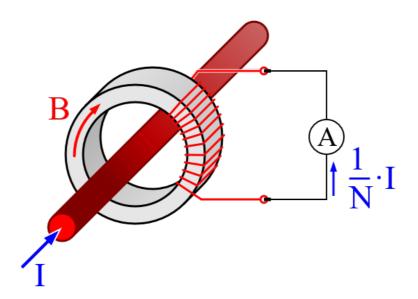
Figure 2.2: Ideal current probe
[2]

There are two types of current probes, injection probes and current monitor probes. These two probe types are very similar but have some differences.

Current Injection Probe

- Designed to inject power into cable.

- Frequency range varies between different probe models. Normally, the frequency range is kHz to hundreds of MHz.

- Maximum power that the probes can be fed with is usually between 75W and 200W.

Current Monitor Probe

- Designed to measure the amount of current flowing through a cable.

- Frequency range varies between different probe models. Normally, the frequency range is kHz to hundreds of MHz.

- Maximum current that the probe can measure is usually a few hundreds of amperes.

Basically, the two probes are very similar. The current injection probe is usually bigger and designed to apply higher power. But both probe types are designed according to Figure 2.2 with a winded core.

2.5   Filter

Since the ground shield can be full of disturbances from other systems, a filter is needed to be able to only look at the signal that has been transmitted from the injection probe. There are several ways to do this.

- **Digital filter:** Digital filtering is pretty simple since we know the frequency of the transmitted signal. The problem with only use digital filtering is that the disturbances can be much bigger than the signal that is to be measured. If that is the case, the ADC can be saturated which means that the sampled signal will be chopped and is hard to process.

- **Analog passive filter:** An analog passive filter works well, but need to be designed for a certain center frequency and amplification since the passive filter attenuate the signal. Since two frequencies should be supported (1kHz and 40kHz) is is hard to do a filter that cover both frequencies without allowing the low frequency disturbances to pass. Two separate filters can be used to cover both the frequencies and a switch to choose which filter that is to be used.

- **Switched capacitor filter:** A switched capacitor filter works like an analog passive filter, but instead of using resistors to set the filter properties, switched capacitors are used. A switched capacitor is a capacitor where MOSFET switches are used to control the flow of charge into and out from the capacitor. By using non-overlapping clocks to control the switches respective, the capacitor can be switched to behave like a resistor. This solution is available as integrated circuits where a clock frequency can be changed to change the center frequency of the filter.[5] Figure 2.3 shows a simple RC Low-pass filter and an equivalent Low-pass filter made using switched capacitors.
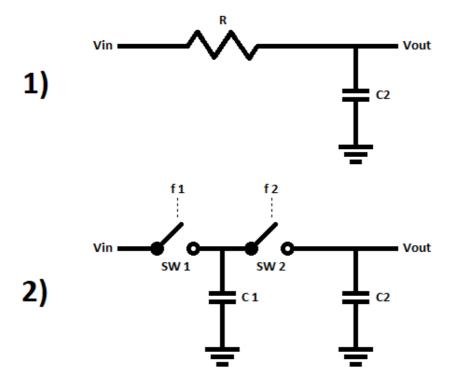
Figure 2.3: Filters: 1) RC low-pass filter and 2) Switched capacitor equivalent low-pass filter

The switched capacitor solution is chosen for this purpose since the filter center frequency can be tuned by the microprocessor to the desired center frequency. This allow the user to change frequency to filter and measure in a spectrum that is full of disturbances depending on the environment the measurement is performed in. Another advantage with the switched capacitor filter is that it minimize the risk of saturating the ADC since it only allow the desired frequency span to pass. To improve the filter, a digital filter can also be applied to make the signal even clearer.

2.6   Battery management system

A battery management system is used to improve the battery life and to protect the battery, the electronics and it's user. A good battery management system has the following functionality:

- **over-charge protection:** When charging a battery, it is important to not overcharge the battery since it can damage or even make the battery catch fire. To prevent this, the battery voltage is monitored and if the battery is going to be overcharged, the charger turns off.

- **over-current protection:** If the load is to high or, in worst case shorted, the BMS disconnect the battery to avoid high current discharge leading to battery damage or damage on the electronics.

- **Temperature monitor:** To avoid overheating or to detect if the battery is broken, the battery temperature is monitored.

- **Balance the cells:** When a battery consists of multiple cells, these cells can have different internal resistance. When charging, this can lead to one cell being overcharged and another cell not being fully charged. To avoid this, the battery cells voltage is measured individually. If one cell is fully charged and another cell is not, the fully charged cell is drained through a resistor and the cells are balanced to have the same amount of charge.

2.7 DC-block

To block the DC current, a capacitor in series is commonly used. The capacitor together with the load resistance implements an RC high-pass filter that blocks the low frequencies and only let the high frequencies pass. Figure 2.4 display a low-pass RC-filter that is equivalent to a capacitor DC-block.
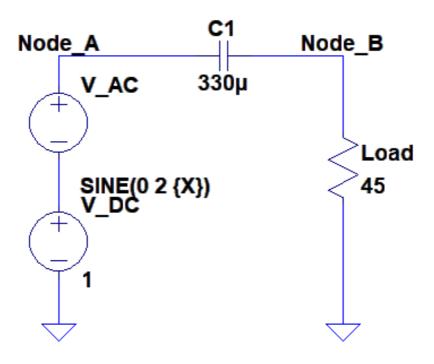
Figure 2.4: DC-block capacitor equivalent RC-filter

Since the filter is not restricted to only block the DC component (0 Hz), low frequencies will be attenuated. The equation for calculating the cutoff frequency for an ideal RC-filter is described in formula 2.2, where f_{-3dB} is the -3dB cutoff-frequency, C is the capacitance and R_{load} is the equivalent resistance of the load the signal will drive.

$$f_{-3dB} = \frac{1}{2\pi C R_{load}}$$
(2.2)

This means that the signal frequency will be attenuated by 3dB. Therefore, the value of the capacitor need to be chosen large enough to not cut off the lowest frequency of interest. Since we only want to block the DC-current (0 Hz) and R_{load} can vary. The capacitance C should be chosen as large as possible.

Figure 2.5 show the simulation result of the RC-filter circuit in Figure 2.4 with ideal components. The simulation result show that the DC-component is removed without any significant attenuation of the AC signal.
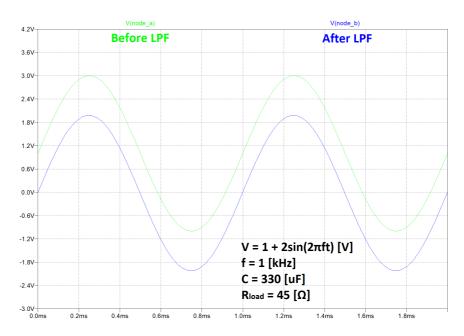
Figure 2.5: LTSpice simulation of RC-filter in Figure 2.4

2.8 Analog switch

To be able to use the same output for two connectors, an analog switch can be used. There are a lot of switches on the market, here are some of them.

- Mechanical relay A mechanical relay is good since it can handle a high current and have a very small impact on the signal. The drawback of using mechanical relays is their slow switch speed, high power consumption and short lifetime.

- Solid-state relay A solid state relay (SSR) is a switching device that use power semiconductor devices to switch currents up to around a hundred amperes. Compared with a mechanical relay, the SSR has much faster switching speed and lower power consumption. But it is more expensive and is at higher risk of overheating when placed crowded on a PCB [7].

- IC switches There are a lot of good IC-switches with low resistance and fast switching speed, but they are temperature sensitive and can only handle a limited amount of power.

2.9 DAC and DMA

The Digital to analog converter (DAC) is using direct memory access (DMA) which means that the DAC is reading the output values directly from the memory without involving the MCU. This way, the MCU don't limit the data rate of the DAC and the MCU can perform work while waiting for a relatively slow I/O data transfer.

9

2.10 Memory

There are several types of memory in most micro-controllers.

- **DRAM**
  DRAM stands for dynamic random access memory and it's used in microcontrollers on the market due to it's fast read and write speed and low cost. DRAM is used to store the stack when executing a program but can't be used for storage since the memory is volatile and loses all data on power reset. The memory cells need to be rewritten multiple times each second to prevent them from discharge and lose the information they store.

- **SRAM**
  SRAM stands for static random access memory. Unlike a dynamic random access memory , the SRAM does not have to be rewritten all the time to store it's information. But it will loose the stored data on a powerloss.

- **EEPROM**
  EEPROM stands for Electrically erasable read only memory and is commonly referred to a NOR-type static memory. It is a good way to store program configuration variables since it's byte-wise erasable and writable. The EEPROM keep the data on powerloss.

- **Flash**
  Flash is a type of EEPROM. It is a NAND-type static memory commonly used to store large data, such as the program binary. It's not recommended to store variables that are changed often in the flash memory since the flash has a limited number of writes in it's lifespan. Flash is also erased and written in sections. This makes you copy the whole section and write it back if only some bytes in the section is to be changed.

2.11 ADC

ADC stands for analog to digital converter. It takes an input voltage and convert it to digital data. This is done by comparing the input voltage with different reference voltages. The number of compares set the resolution of the ADC. Normally, the resolution is between 8-bit and 16-bit. But there is ADCs with much higher resolution on the market. Higher resolution makes the sample time longer and the input and reference voltages must have very low noise to make use of the extra resolution bits.

3 Design of Loop Impedance Measurement Tool

3.1 Measure Impedance

The measurement can be simplified and explained using Figure 3.1. We have the following variables:

V_{TX} is the voltage from the sinus signal generator that goes in to the transmitting probe.

z is the complex shield transfer impedance.

V_{RX} is the measured voltage at the receiver probe.
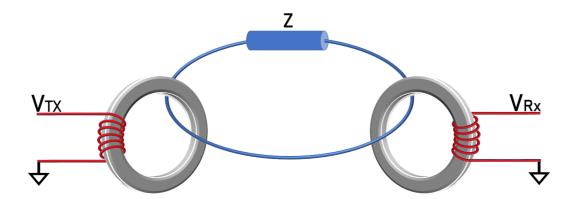
Figure 3.1: Measurement setup

The signal generator generates an AC signal described in formula 3.1, where A is the amplitude, f is the frequency, and t is the time.

$$V_{TX} = A sin(2\pi f t) \tag{3.1}$$

Since we have inductance in the probes, and even in the shield, the difference in phase between V_{TX} and V_{RX} have to be considered. To do this, we mix V_{TX} and V_{RX} with I, given from Equation 3.2 and Q, given from Equation 3.3.

$$I = cos(2\pi f t) \tag{3.2}$$

$$Q = sin(2\pi f t) \tag{3.3}$$

This gives the us $V_{TXcomplex}$ and $V_{RXcomplex}$ displayed in Equation 3.4 and Equation 3.5.

$$V_{TXcomplex} = V_{TX}I + jV_{TX}Q \tag{3.4}$$

$$V_{RXcomplex} = V_{RX}I + jV_{RX}Q \tag{3.5}$$

The quotient of $V_{TXcomplex}/V_{RXcomplex}$, shown in Equation 3.6 will be independent of the amplitude of the signal generator and only vary depending on the loop impedance and the characteristics of the two probes. The transfer impedance of the probes varies with the frequency f of the sine wave.

$$A_{complex} = \frac{V_{TXcomplex}}{V_{RXcomplex}} \tag{3.6}$$

By using Kirchhoff's voltage law (KVL), the circuit can be explained by Equation 3.7. $Z_{TXcomplex}$ is the transfer impedance for the injection probe with cable losses and signal generator characteristics included.
$Z_{complex}$ is the unknown complex shield transfer impedance.
$Z_{RXcomplex}$ is the transfer impedance for the receiving probe with cable losses and receiver characteristics included.
I is the current in the shielded cable.

$$0 = V_{TXcomplex} - (Z_{TXcomplex} + Z_{complex})I - V_{RXcomplex} \tag{3.7}$$

Rewrite Equation 3.7 to Equation 3.8.

$$V_{TXcomplex} = (Z_{TXcomplex} + Z_{complex})I + V_{RXcomplex} \tag{3.8}$$

Rewrite Equation 3.8 to Equation 3.9 using ohms law $V_{RXcomplex} = Z_{RXcomplex}I$.

$$V_{TXcomplex} = (Z_{TXcomplex} + Z_{complex})I + Z_{RXcomplex}I \tag{3.9}$$

Rewrite Equation 3.9 to Equation 3.10.

$$V_{TXcomplex} = I(Z_{TXcomplex} + Z_{complex} + Z_{RXcomplex}) \tag{3.10}$$

Divide both sides of Equation 3.10 by I and get Equation 3.11.

$$\frac{V_{TXcomplex}}{I} = (Z_{TXcomplex} + Z_{complex} + Z_{RXcomplex}) \tag{3.11}$$

Rewrite Equation 3.11 to Equation 3.12 using ohms law $I = \frac{V_{RXcomplex}}{Z_{RXcomplex}}$.

$$\frac{V_{TXcomplex}}{V_{RXcomplex}} Z_{RXcomplex} = (Z_{TXcomplex} + Z_{complex} + Z_{RXcomplex}) \tag{3.12}$$

Using Equation 3.6 and Equation 3.12, we get Equation 3.13.

$$A_{complex} Z_{RXcomplex} = (Z_{TXcomplex} + Z_{complex} + Z_{RXcomplex}) \tag{3.13}$$

Division by $Z_{RXcomplex}$ gives Equation 3.14.

$$A_{complex} = \frac{Z_{TXcomplex} + Z_{complex} + Z_{RXcomplex}}{Z_{RXcomplex}} \tag{3.14}$$

Split Equation 3.14 to receive 3.15.

$$A_{complex} = \frac{Z_{complex}}{Z_{RXcomplex}} + \frac{Z_{TXcomplex} + Z_{RXcomplex}}{Z_{RXcomplex}} \tag{3.15}$$

This can be written as a linear dependency shown in Equation 3.16. z is the unknown impedance in the shield that is to be calculated. α and β is frequency dependant constants.

$$A_{complex} = \alpha z + \beta \tag{3.16}$$

Equation 3.16 can be rewritten to a linear function that describes the unknown impedance z as a function of $A_{complex}$. This is shown in Equation 3.17, where k and m are calibration constants.

$$z = k(A_{complex}) + m \tag{3.17}$$

By doing two measurements where z is known, we get the two calibration constants k and m. These two calibration constants are dependent on the characteristics of the probes, the frequency used, the injection loss of the cables between the probe and the instrument, and internal losses in the instrument. Since the calibration constants are frequency dependant, the calibration and measurement has to be done with a fixed frequency f.

Impedance is a complex number describing both the magnitude and phase. The magnitude represents the resistance and the phase represents the capacitance and inductance. In this application, the resistance is the interesting part of the impedance. The capacitance will be negligible and the inductance will be very small if the measurement frequency is low enough. The measurement result will though be complex since the current probes are inductive.

Laboratory work

To verify the method, some laboratory work was done. Loops were made using singe core wires that were measured by applying a current in each end, while measuring the voltage over the wire. By using Omhs law, the resistance of the wire was calculated. Each of the wires were then soldered to a loop. The loops are displayed in Figure 3.2
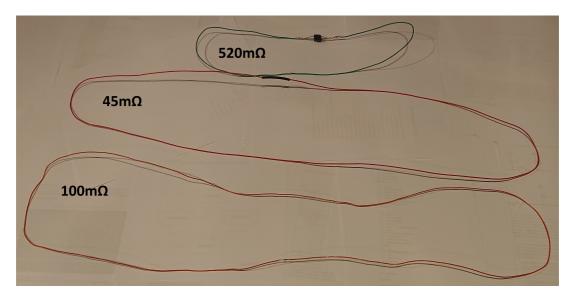
Figure 3.2: Loops with measured resistance

Each loop were measured by applying two current probes, one connected to a signal generator and an oscilloscope and one connected only to the oscilloscope. The two signals from the probes were then measured and imported to MATLAB to make the calculations. Several measurements were made with different loops, frequency and amplitude. The laboratory setup is shown in Figure 3.3
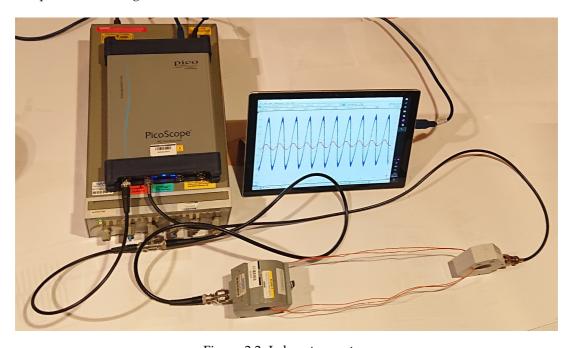
Figure 3.3: Laboratory setup

3.2 Current probe fail detection

When the current probes are installed on the DUT, there is a risk that a current probe is not fully closed. This is important to detect to avoid faulty measurements. If the injection probe is open, the impedance of the probe will increase and the voltage will drop. One simple way to detect this is to use two equal probes and measure two times with swapped injection port and measurement port. This way, you get two results that should be equal. If the results differ, it is an indication that one of the probes is not closed correctly. The probes can be of different model. But in that case, the calibration need to be done two times with different current direction. So there is one calibration for each direction.

3.3 Voltage probe

By adding a voltage probe, the voltage drop over a specific part of the loop can be measured. This allows the user to measure the voltage drop over a specific connector, to evaluate the conductivity in the connector, in case of high loop impedance. This is illustrated in Figure 3.4.
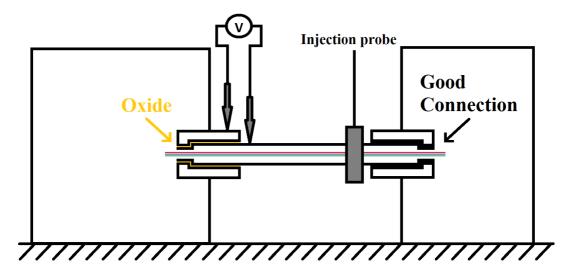
Figure 3.4: Voltage probe setup

3.4 Design alternatives

Requirements

The design have the following minimum requirements:

- 80MHz system clock

- 512KB RAM

- 3x ADC (12-bit, 1MS/s)

- 1x DAC (8-bit, 1MS/s)

- 1x DAC/Clock timer (at least 1MHz)

- 1x I2C

- 1x UART

- 10x I/O ports

- Display support

One PCB solution

The one PCB solution is a PCB design where all necessary hardware are located on one single PCB. The microprocessor chosen in this solution is STM32G474CE which is a 170MHz 32-bit ARM processor (package LQFP 48). See circuit diagram in Figure 3.5.

Figure 3.5: STM32G474CE

Advantages of this solution:

- The ADCs and DACs can be placed close to the connectors to avoid EMC problems.

- The PCB design can be made to fit a certain pre-designed case.

- If more units are manufactured in the future, there is less dependency of dealers.

- Components that are commonly used on SAAB Dynamics can be used.

Disadvantages of this solution:

- Bigger PCB design which takes longer time to design.

- A mistake in the PCB design can delay the whole project by weeks.

- A separate programmer is needed.

- Can be more expensive in small quantities.

- Need to be soldered in oven with stencil or by the manufacturer.

Zynq module with motherboard

The Zynq platform is commonly used on Saab Dynamics and is a powerful Dual-core ARM processor with an FPGA. It is able to run Linux OS and works well for the most demanding applications. A Zynq module that SAAB Dynamics has developed based on Zynq-7000 SoC could be used together with a custom PCB containing filters, battery management system, connectors and user interface.

The circuit diagram for Zynq-7000 is shown in Figure 3.6.
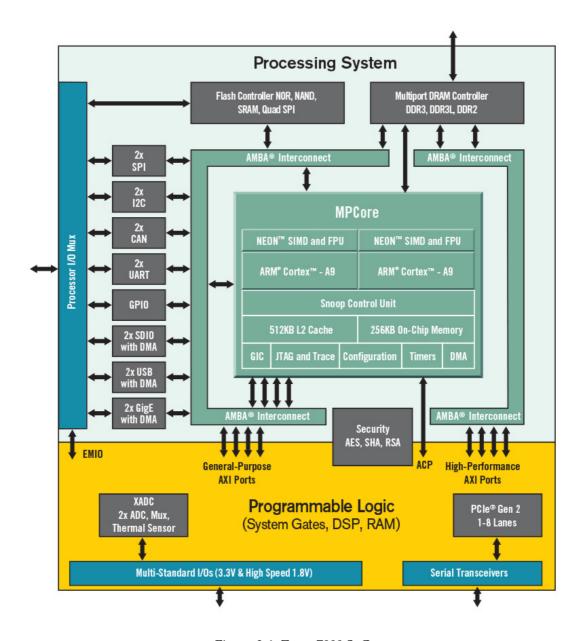
Figure 3.6: Zynq-7000 SoC

Advantages of this solution:

- Very powerful

- Well known development platform on SAAB Dynamics.

- The FPGA makes it possible to control the sampling rate on clock basis.

Disadvantages of this solution:

- The Zynq platform is unnecessary powerful for this application.

- Expensive.

ST Development module with shield

The STM32H747I-DISCO is a complete demonstration and development kit. This kit, displayed in Figure 3.7, could be used together with a custom PCB shield where the connectors, filters and battery management system are located.

Figure 3.7: STM32H747I-DISCO Discovery kit

Figure 3.8 show the circuit diagram for STM32H747XI which is the microprocessor on STM32H747I-DISCO.

System		
SMPS, LDO, USB and backup regulators POR/PDR/PVD/BOR		
Multi-power domains		
Xtal oscillators 32 kHz + 4 ~48 MHz		
Internal RC oscillators 32 kHz + 4, 48 & 64 MHz		
3x PLL		
Clock control		
RTC/AWU		
1x SysTick timer		
2x watchdogs (independent and window)		
82/114/140/168 I/Os		
Cyclic redundancy check (CRC)		
Unique ID		

Control
2x 16-bit motor control PWM synchronized AC timer
10x 16-bit timers 2x 32-bit timers
5x Low-power timer
16-bit High res. timer

Chrom-ART Accelerator™

JPEG Codec Acceleration

Cache I/D 16+16 Kbytes

Arm® Cortex® -M7 480 MHz

+

Arm® Cortex® -M4 240 MHz

Floating point unit (DP-FPU)

Nested vector interrupt controller (NVIC)

JTAG/SW debug/ETM

Memory Protection Unit (MPU)

ROP, PC-ROP anti-tamper

AXI and Multi-AHB bus matrix

4x DMA

True random number generator (RNG)

2-Mbyte dual-bank Flash memory

RAM 1056KB incl. 64KB ITCM

FMC/SRAM/NOR/NAND/ SDRAM

Dual Quad-SPI

1024-byte + 4-Kbyte backup SRAM

Connectivity
TFT LCD controller
MPI-DSI
HDMI-CEC
6x SPI, 3x I²S, 4x I²C
Camera interface
Ethernet MAC 10/100 with IEEE 1588
MDIO slave
2x FDCAN (Flexible Data rate)
1x USB 2.0 OTG FS/HS
1x USB 2.0 OTG FS
2x SDMMC
4x USART + 4 UART LIN, smartcard, IrDA, modem control
1x Low-power UART
4x SAI (Serial audio interface)
SPDIF input x4
DFSDM (8 inputs/4 filters)
SWP (Single Wire Protocol)

Analog
2x 12-bit, 2-channel DACs
3 x 16-bit ADC (up to 3.6 Msps) 20 channels/up to 2 MSPS
Temperature sensor
2x COMP
2x OpAmp

Figure 3.8: STM32H747XI

The advantages of this solution is:

- Programming and debugging interface and power regulator included on the board.

- Powerful 480MHz ARM micro-controller with 1MB RAM.

- Display with driver included.

- Possible to use both capacitive touch display and buttons as user input interface.

- High resolution 16-bit ADCs and DACs with sample rate > 2Ms/s.

- Works standalone right out of the box.

- ST have a collections of example software that works with the kit.

- The custom PCB will be simple to manufacture and can be soldered by hand.

- Standard Arduino Uno layout of the shield connectors, resulting in that the custom PCB can be used with multiple development kits from ST or Arduino.

The disadvantages of this solution is:

- Overqualified micro-controller for this purpose.

- Expensive if manufactured in large quantities.

- The developing environment are not commonly used on SAAB Dynamics.

- The solution will result in long traces between the ADC ports on the processor and the connectors.

- Less opportunities to choose which I/O ports to use.

- The Discovery kit includes a lot of extra hardware support that is not necessary for this application.

- The case of the tool need to be customized to fit the electronics in a good way.

Chosen design solution

The choice of design alternative depends on where one want to put the majority of effort in the project. The Zynq platform will require a lot of effort in learning the development environment, while the one PCB solution will put the majority of effort in PCB design and hardware testing. The Discovery kit will speed up the design process and allow more time to be put on making the application really good. Instead of using time to write display driver, premade display drivers can be used to design a graphical user interface with touch that displays data in graphs.

The best solution is the Discovery kit with a custom PCB since this solution will reduce development time of hardware and software. This solution gives full compatibility since most of the required hardware is on the Discovery kit and the missing hardware can easily be added on the other PCB. Another advantage of this solution is that there is a lot of software examples and guides on how to use the integrated development environment. The one PCB solution is also good, but will require more time on hardware design and testing. Since the one PCB solution takes more time, there will be no time to implement a graphical display, instead a simple character display is to be used.

3.5 Components

The following components is needed to get the required hardware functionality.

- Battery and battery management system
- Power amplifier
- Filter
- Output switch
- ESD protection diodes
- Connectors
- DC voltage regulator

Battery and battery management system

To power the tool, a battery solution is needed, which also need to be charged with a charger or battery management circuit.

Battery

The battery should be rechargeable and easily replaceable. Therefore, two 18650 Li-Ion battery are used. These batteries are common on the market and have a cell voltage of 3.7V. Since the maximum required voltage in the circuit is 7V, two Li-Ion battery cells are used in series. Li-Ion can give high current which is good since it won't limit the output of the power amplifier. This solution also makes it possible to use the node between the two cells as a virtual ground which is good for adding an offset to the input signal of the power amplifier.

Battery management system

To monitor the health of the batteries and charge the batteries, a battery management system (BMS) is required. The chosen solution is to use a BQ25887R integrated-circuit from Texas instrument. This BMS circuit has a lot of good functionality.

BQ25887R functionality

- 5V input
- 2 cell LI-Ion compatibility
- Cell balancing
- Small size
- Thermal monitoring
- I2C communication

The 5V input voltage is perfect since it's the same voltage as the USB-standard uses. This makes it easy to use a smartphone charger as power supply. Since the node between the two battery cells can be used as a virtual ground, there is a risk that the cells will be discharged unequally. Unbalanced cells can decrease the lifetime of the battery cells since one cell can be overcharged while the other cell is uncharged. Therefore, a cell balancing system is good to have. The BMS monitor cell voltages, temperature and charging current to make sure the batteries are healthy. The microprocessor can write settings to the BMS and get battery and charging status via I2C communication interface.

Power amplifier

Since the frequency used is relatively low ($<$ 100kHz) there is a lot of audio amplifier solutions which are designed for this frequency span. The amplifier chosen is TPA3116D2 which is a 10W stereo amplifier from Texas Instruments. Since we only need one channel, this amplifier is configured in bridge mode, which merge the two channels to get higher output power. The Output in bridge-mode configuration is 18W with 8 Ohm Load. This Class D amplifier is good since it has small package and does not require large inductors like most other audio amplifier circuits do.

Filter

The filter is designed using a LTC1068-25 integrated circuit from Linear Technologies. This circuit has the advantage of using switch capacitors which makes it frequency tunable. This circuit is available in LT-Spice, which makes it easy to simulate a good design for our application.

Since the received signal can have a low amplitude, a Low noise amplifier is needed to pre-amplify the signal so the ADC can sample with good resolution. For this application, a MCP6S21 programmable gain amplifier (PGA) is used. This PGA can be configured using SPI to get the correct gain.

Output switch

To be able to switch the output ports, two mechanical relays are used. The relays chosen is the AGQ200S03 which is a small surface mounted mechanical relay. The mechanical relay solution doesn't affect the signal as much as a solid state relay, which makes it useful in this application. The disadvantage of using a mechanical relay is the power consumption. But it is no problem in this application since the relay is only on for a short period of time.

ESD protection diodes

To protect the connector from electrostatic discharge (ESD), some TVS diodes is used. These diodes are placed close to the connectors and have the functionality to shorten all electrostatic pulses to ground that can occur if someone is touching the connectors. By attenuating the pulses, damage of the micro-controller and filter circuit is prevented.

Connectors

The connector used for charging is a USB-C. This connector is commonly used as a smart-phone charger connector. The probes are connected with BNC-connectors which are commonly used in similar applications, are shielded and cheap compared with the N-connectors. To connect the battery, a simple terminal block is used.

DC voltage regulator

Since the power amplifier requires a stable voltage to have a constant gain, a low-dropout regulator is used to keep the voltage stable at 7V. The disadvantage of this solution is the low efficiency compared with a switched regulator. The advantage is the low cost, stable voltage and that it doesn't require a lot of passive components.

3.6 Hardware design

Schematic

The schematic is divided into several sheets which are connected to each other through ports and power nets. The purpose of this division is to make the schematic easier to read and design.

STM32H747-DISCO docking connector

The development board STM32H747-DISCO is docked to the PCB through 4 headers. The headers are positioned according to the Arduino standard which makes it possible to change the development board to another Arduino compatible board if the new board meets the requirements for each used pin. The schematic over this connector is displayed in Figure 3.9 and show which pins that are used for each purpose. Figure 3.10 show the hardware functionality on each pin in the docking connector.
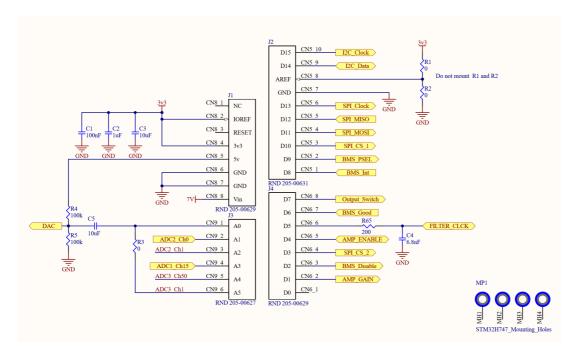

Figure 3.9: Schematic of the docking connectors for the STM32H747-DISCO

Table 10. ARDUINO® Uno V3 compatible connectors

CN No.	Pin No.	Pin Name	MCU Pin	Function		Function	MCU Pin	Pin Name	Pin No.	CN No.
						I2C4_SCL	PD12	D15	10	CN5 Digital
						I2C4_SDA	PD13	D14	9	
		-				AVDD	-	AREF	8	
						Ground	-	GND	7	
CN8 Power	1	NC	-	-		SPI5_SCK	PK03	D13	6	
	2	IOREF	-	3.3 V Ref		SPI5_MISO	PJ11	D12	5	
	3	RESET	NRST	RESET		TIM1_CH2N, SPI5_MOSI	PJ10	D11	4	
	4	+3V3	-	3.3 V$^{(1)}$ input / output		TIM1_CH1, SPI5_NSS	PK1	D10	3	
	5	+5V	-	5 V output		TIM8_CH2	PJ6	D9	2	
	6	GND	-	Ground		-	PJ5	D8	1	
	7	GND	-	Ground				-		
	8	VIN	-	Power input$^{(2)}$		-	PJ0	D7	8	CN6 Digital
		-				TIM8_CH2N	PJ7	D6	7	
CN9 Analog	1	A0	PF7	ADC3_IN5		TIM3_CH1	PA6	D5	6	
	2	A1	PF10	ADC12_IN0		-	PJ4	D4	5	
	3	A2	PA0_C	ADC12_IN1		TIM13_CH1	PF8	D3	4	
	4	A3	PA1_C	ADC1_IN15		-	PJ3	D2	3	
	5	A4	PC2_C or PD13	ADC3_IN50 or I2C4_SDA$^{(3)}$		UART8_TX	PJ8	D1	2	
	6	A5	PC3_C or PD12	ADC3_IN1 or I2C4_SCL$^{(3)}$		UART8_RX	PJ9	D0	1	

Figure 3.10: Table 10 from the STM32H747-DISCO User Manual displaying the functionality on each pin on the docking connector [10]

Battery management system

To be able to charge the battery and monitor the state of the battery, a battery management integrated circuit from Texas Instruments is used. Figure 3.11 show the schematic of how this IC is used. The IC get the charging power from the USB-C port shown in Figure 3.16. It then charges the two batteries which are connected in series between GND and the 7v4-node. Between the two cells, there is a node called 3v7, which is used to balance the two cells. The status of the batteries is sent over a SPI-interface to the STM32 Microcontroller. The schematic also contain a 7V regulator which is used to give a stable 7V supply voltage to the power amplifier.
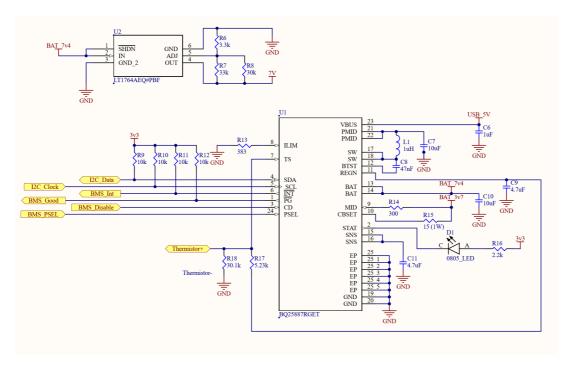

Figure 3.11: Schematic of the Battery management system

Power Amplifier

The power amplifier in the schematic shown in Figure 3.12 is an audio amplifier. This is an easy and simple solution. Since the frequency used to feed the injection probe is close to the frequency span used in audio applications, the audio amplifier circuit is compatible with the application of this master's thesis. The audio amplifier is used in bridge mode, which is when both channels are merged to only be able to play mono-sound but with close to the double output power.
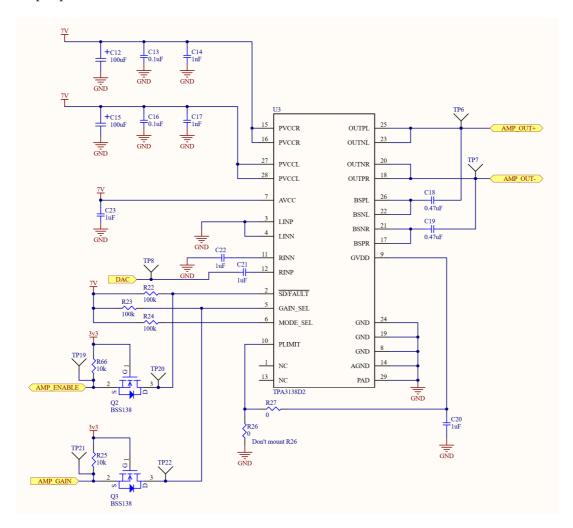

Figure 3.12: Schematic of power amplifier

Filter

Two identical filters are used, one for each ADC input. The schematic of the filter is shown in Figure 3.13 and is built by a quad 2nd order building block. The filter is a 8th order switched capacitor filter. The center frequency can be swept between 1kHz and 100kHz. Since the filter attenuates the signal, a programmable gain amplifier is used to amplify the signal and add an offset of 1.65V so the ADC can read it.
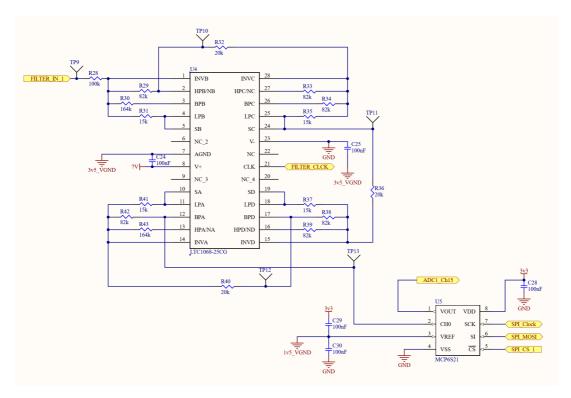

Figure 3.13: Schematic of one of the two identical filter circuits

Figure 3.14 and Figure 3.15 show the LTspice simulation of the filter without the PGA part at different frequencies. The amplitude of the input signal is an estimation based on measurements done with two current probes, a signal generator and an oscilloscope.

Figure 3.14: LTSpice simulation of filter with signal input frequency 1kHz and filter clock set to 10kHz
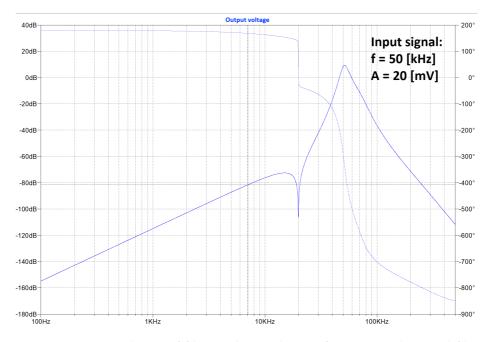

Figure 3.15: LTSpice simulation of filter with signal input frequency 50kHz and filter clock set to 500kHz

Connectors and voltage references

The schematic in Figure 3.16 shows all external connectors except the docking header for the STM32 development board. The sensitive connectors are ESD protected with TVS-diodes close to the connector inputs. This is to prevent damage in case of an electrostatic discharge from a finger ect. The USB-C port is configured to be detected from the host as a 2.4A charging port. To be able to switch the output connectors, two mechanical relays are used. This gives the functionality to detect if one probe is not closed correctly. The schematic also contains two voltage dividers. This is to set the reference voltages used in the amplifiers to get the correct offset since the ADC and power amplifier only can read positive voltages.
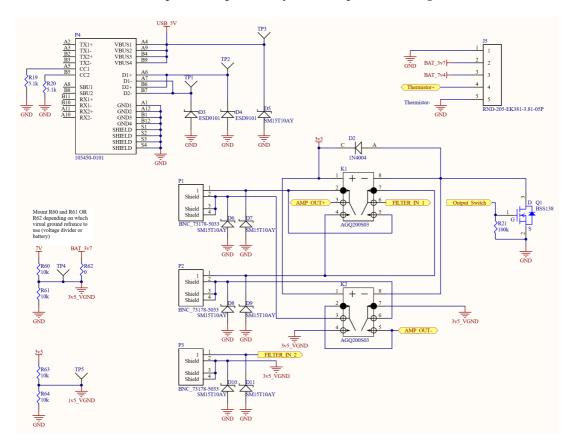

Figure 3.16: Schematic of external connectors, except the STM32H747-DISCO docking headers, and voltage references

32

Layout

The layout has been designed in Altium Designer. The PCB has four layers.

- **Layer 1:** This layer is the top layer which contains signal traces and all components to make the assembly easier.

- **Layer 2:** This layer is a ground plane.

- **Layer 3:** This layer is splitted into several planes which are used to supply different voltages to the components.

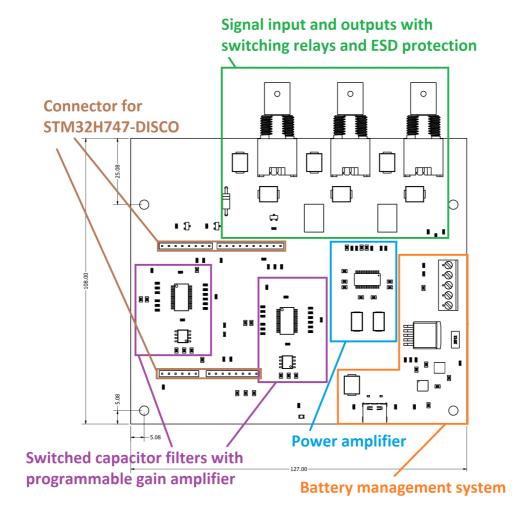- **Layer 4:** This is the Bottom layer, which contains signal routes.

Figure 3.17: Overview of the designed circuit board.

3.7 Software

IDE-Software TouchGFX

TouchGFX is a development environment for STM32 graphical applications. It is drag and drop based, in the same way as the tools included for .NET in Microsoft visual studio. The drawback of TouchGFX is that it has bad hardware access, which makes it hard to write the background applications that communicates with the external hardware. TouchGFX generates a RTOS based C++ application while other IDEs for STM32 often use bare C programming.

Real-time operating system

The application is based on FreeRTOS which is a real-time operating system. This allow the application to run in tasks with an operating system that jumps between the different tasks depending on the priorities of the tasks. The user will experience this like the tasks are performed at the same time, but since only one core is used, in fact the RTOS jumps between the tasks and only runs one operation at a time.[9]

Graphical user interface

The Graphical user interface are displayed on a 4" touch display. This is not the focus on this master's thesis work and is therefore made as simple and functional as possible. The GUI is made as 4 separate screens, which the user navigates between as displayed in Figure 3.18. Each screen has it's own C++ class. To make the screens communicate with each other, there is a class called model, which the different screen classes call to transfer data between the screens.
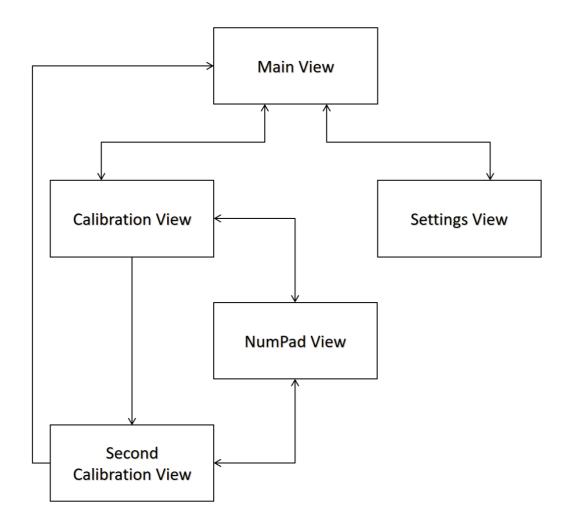
Figure 3.18: Overview of the different views on in the GUI and how the user can navigate between them

From the main screen, displayed in Figure 3.19, the user can run measurements and navigate to calibration and settings screen.

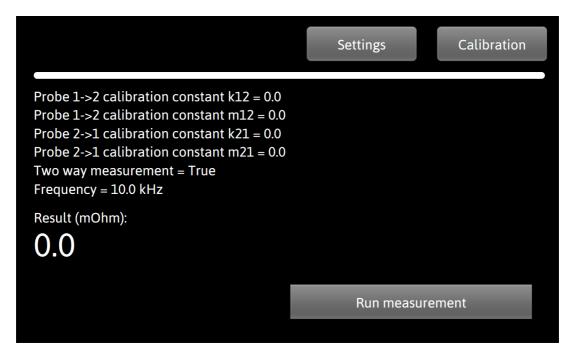Figure 3.19: Graphical design of the main view

The settings screen, seen in Figure 3.20, makes it possible to change measurement frequency and enable or disable two way measurement. When two way measurement is enabled, two measurements are made in total and the input and output ports are switched between the measurements to detect if one of the probes is open.
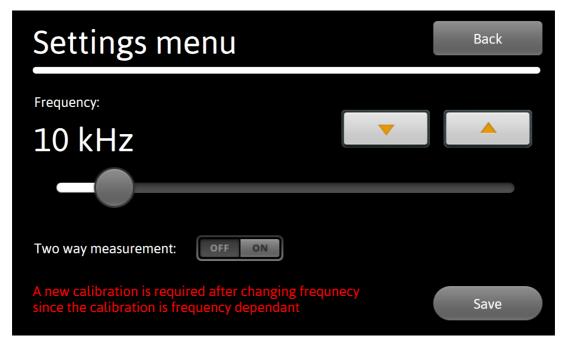

Figure 3.20: Graphical design of the settings view

The calibration menu was split into two views due to lack of space. Figure 3.21 shows the first calibration view, this menu can be used to enter the calibration constants if they are known to the user. Pressing one of the set buttons will navigate to the numpad screen asking for input. If the calibration constants are unknown, which is the most common case, the user can press "Calculate calibration menu" to navigate to the second calibration view.
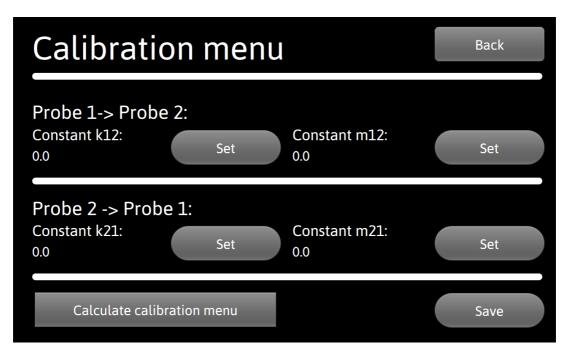

Figure 3.21: Graphical design of the calibration view

The second calibration view shown in Figure 3.22 is used to calibrate the device. The user can simply calculate the constants by doing two measurements on known impedance's.
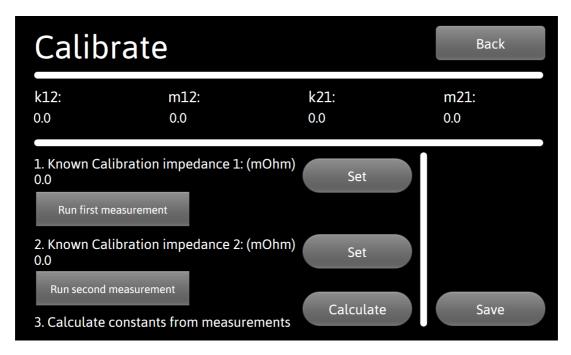
Figure 3.22: Graphical design of the second calibration view

37

This numpad screen, shown in Figure 3.23, is used to get input data. This makes possible for the user to enter an exact value in an easy way.

Figure 3.23: Graphical design of the numpad view

Back-end application

The back-end application is an RTOS task which handles the interaction with all hardware except the touch screen. This task performs the measurements by configuring and enabling the DAC and ADCs. It also controls all the GPIO pins. Most of the calculations are also done in the back-end task.

3.8 System design

The system is designed to have all the required functionality. The base of the system design is a STM32H747 development board from ST Microelectronics. This board is very powerful but is supplemented by another board with some analog filters, amplifiers and a battery management system.

Functionality

- 4 inch touch display

- USB communication interface

- 2 cell Li-Ion battery

- Balanced battery charger

- Battery temperature monitor

- 8-bit DAC for sine wave generation (1kHz - 100kHz)

- 20W power amplifier

- 3x 12-bit ADC

- 2x Adjustable band-pass filter (1kHz - 100kHz center frequency)

- 2x Programmable gain amplifier

- Relay controlled output (to be able to switch injection and monitoring probe)

- Support for Ethernet communication

- Support for Real-time clock (RTC)

The System diagram of the design is displayed in Figure 3.24. All the hardware is implemented, but there is no software for the USB-communication and the voltage probe measurement.
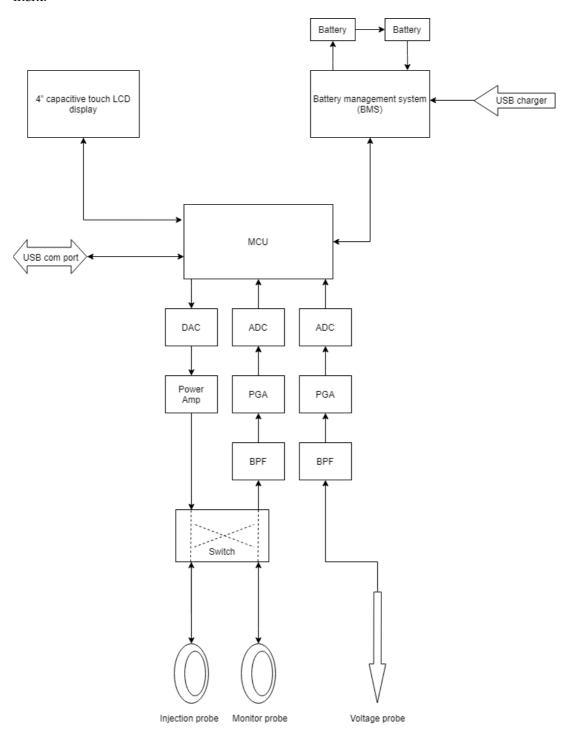
Figure 3.24: System diagram

3.9 Prototype

Figure 3.25 and Figure 3.26 shows the final prototype. In the bottom, there is a 3D-printed box containing two battery cells, two fuses and a 2-pole power switch. The box is then connected with wires to the PCB where the filters, the amplifier and all connectors are located. On top of this, the evaluation board is docked.

Figure 3.25: Assembled PCB

Figure 3.26: Final prototype

The Prototype should be equipped with two current probes as shown in Figure 3.27. In the figure, there is a third BNC connector that is not in use. It is the port for the voltage probe that can be used to measure the voltage over a specific part of the loop.
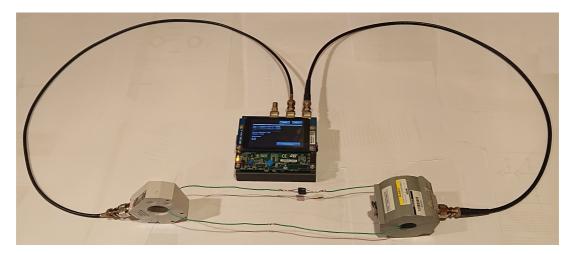
Figure 3.27: Final prototype equipped with current probes

4 Measurement Results

4.1 Laboratory work

Figure 4.1 shows four measurements made with $100\text{m}\Omega$ loop impedance and a 10kHz sine wave as input. The amplitude of the sine wave differs between the measurements.
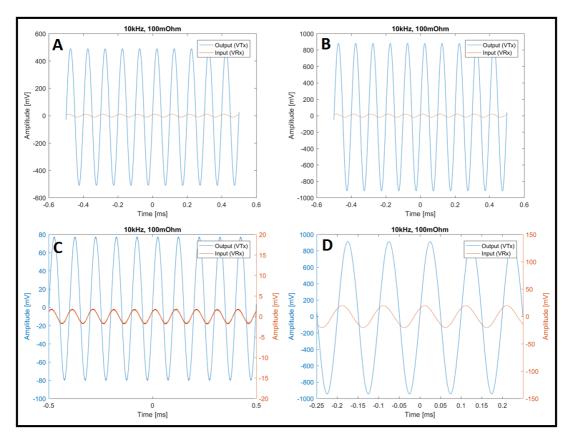
Figure 4.1: Four measurements with z = $100\text{m}\Omega$, V_{Tx} = 10kHz sine with various amplitudes

$A_{complex}$ was then calculated for each measurement. The results are shown in Table 4.1.

Table 4.1: A calculations from data in Figure 4.1

Measurement	A	B	C	D
A_{real}	44.6597	44.7186	44.6111	44.6810
A_{imag}	11.1039	11.0329	11.1207	12.8033

The same measurement was then made with 45mΩ and 520mΩ loop impedance, which can be seen in Figure 4.2 and Figure 4.3.
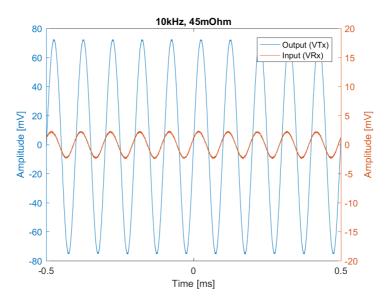
Figure 4.2: Measurement with z = 45mΩ, V_{Tx} = 10kHz sine wave

Figure 4.3: Measurement with z = 520mΩ, V_{Tx} = 10kHz sine wave

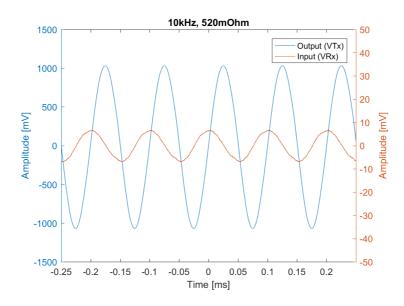By calculating $A_{complex}$ for each of the measurements and then plot the real part of the values against the known resistances of each measurement, the linear dependency can be proven. This is shown in Figure 4.4.
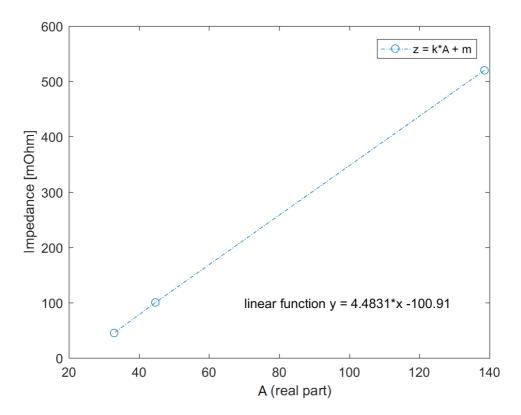
Figure 4.4: Plot of calculated A_{real} from measurement data

The calibration constants is calculated with the result of two measurements, which is shown in Figure 4.5.

$$Z_1 = 520 * 10^{-3}\Omega$$

$$A1_{1(real)} = 138.5435$$

$$Z_2 = 100 * 10^{-3}\Omega$$

$$A_{2(real)} = 44.6810$$

$$k = \frac{abs(Z_1 - Z_2)}{abs(A_{1(real)} - A_{2(real)})} = \frac{abs(520 - 100)}{abs(138.5435 - 44.6810)} = 0.0045$$

$$m = Z_1 - k * A_{1(real)} = 520 * 10^{-3} - 0.0045 * 138.5435 = -0.0999$$

Figure 4.5: Calculation example of the calibration constants using measurement data

The calibration constants can then be used to calculate an unknown loop resistance, which can be seen in Figure 4.6.

$$z = k * A_{3(real)} + m$$

$$A_{3(real)} = 32.8908$$

$$z = 0.0045 * 32.8908 - 0.0999 = 0.0481\Omega = 48m\Omega \approx Z_3 = 45m\Omega$$

Figure 4.6: Calculation example with measurement data from a loop with resistance = 45mΩ

The measurement error in these measurements is $\frac{|45-48|}{|45|} = 6.6\%$

4.2 Hardware evaluation

Several measurements were made to evaluate the function of hardware.

Power Amplifier

The power amplifier was tested without the STM board using a signal generator and an oscilloscope. The result is displayed in Figure 4.7.
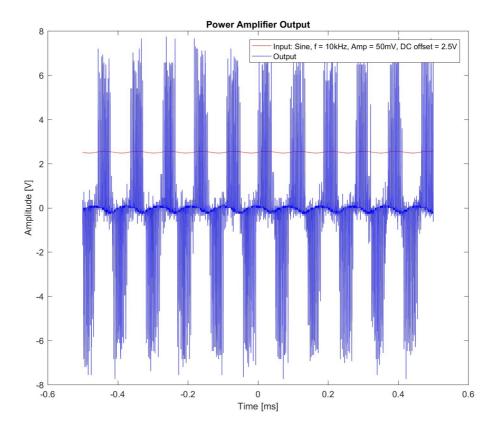
Figure 4.7: Power Amplifier measurement with fixed input $V_{in} = 2.5 + 0.05 * sin(2\pi 10000)$ V

47

The power amplifier was then further evaluated by adding two current probes and a ground loop with a known resistance of 100mΩ. This measurement is displayed in Figure 4.8.
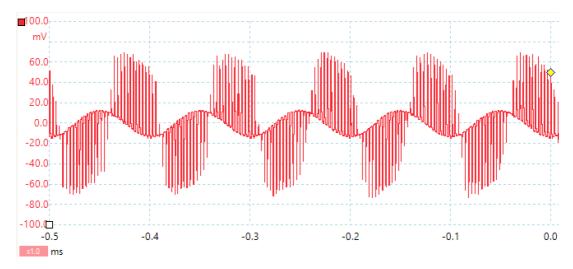
Figure 4.8: Power Amplifier measurement in time domain with two current probes and a 100mΩ ground loop

To be able to see the harmonics better, the FFT of the result is displayed in Figure 4.9.
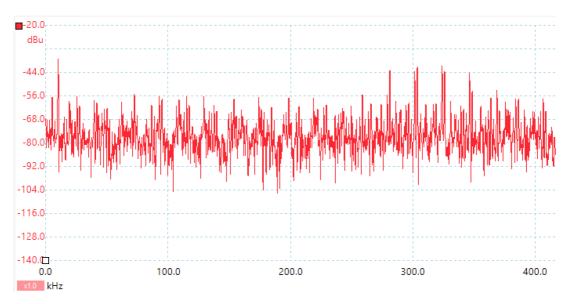
Figure 4.9: Power Amplifier measurement in frequency domain with two current probes and a 100mΩ ground loop

Filters

The filter was tested separately by applying a signal generator on the input and measuring between the filter and the PGA with an oscilloscope. This measurement is a bit tricky since the oscilloscope and the signal generator can't share the same ground since the input use a virtual ground as reference. The measurement result can be seen in Figure 4.10. The attenuation is 21dB, which is more than expected from the simulations.
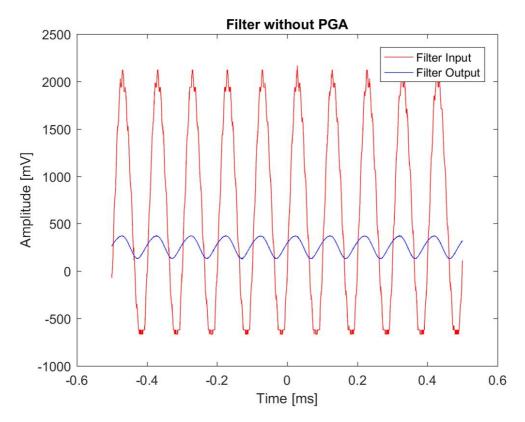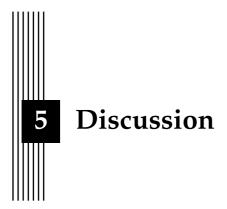
Figure 4.10: Input filter measurement with 10kHz noisy sine wave as input

5 Discussion

5.1 Laboratory work

The laboratory work shows that the loop impedance is possible to measure with good enough measurement accuracy. The measurement results in the labs are close enough to reveal oxidized connectors or damaged shields.

5.2 Power switch

Some mistakes were made during this thesis work. One mistake is that the power button is missing in the schematic. A power switch and two fuses were added between the two batteries and the BMS. The switch turn off the device and prevent the batteries from draining when not used. The problem with this is that the device can't be charged while turned off. It is also a possibility to modify the PCB and install a switch between the regulator and the development board. This is a bit advanced to do since the power plane in the middle of the PCB has to be cut off.

5.3 PCB test pads

The PCB-layout was designed with test pads on all important nodes to make troubleshooting easy. The mistake done was to put these test pads on the top layer, which makes them hard to reach with the probes when the STM32 development board is docked. These test pads are very good to have, but they should have been placed on the bottom layer, or on both layers, for easy access.

5.4 Power amplifier

The Amplifier used is a class D amplifier. A class D Amplifier is good for audio applications since it has good efficiency compared with class A and B amplifiers. A class D amplifier use Pulse width modulation (PWM) to generate the output. This works for speakers, but is not good for this application. A sine wave generated using PWM contains a lot of harmonics which will follow through the whole measurement. This cause problems since the calculation model used is simplified by assuming a fixed frequency. The amplifier will therefore prevent the tool from being able to perform reliable measurement.

5.5 Filter design
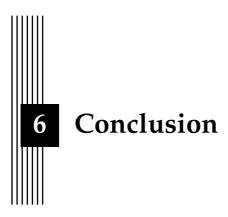
The Filters will filtrate the incoming signal, but the attenuation is too large. This will cause problems since high PGA gain will cause noise. A better solution would have been to amplify the signal both before the filter and after, or design a filter with less attenuation.

5.6 Battery management system

The battery management system worked well, but the I2C communication to allow the MCU to read the battery voltage was never implemented in the software.

5.7 STM32 evaluation board

The STM32 board used was new on the market and has two cores. This resulted in a lot of complications since the software development tools for STM32 mainly only support one core devices. This made the software development to take much longer time than expected and limited the debug possibilities.

6 Conclusion
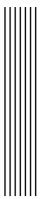
Some parts of the master's thesis have been successful while other parts are to be seen as a learning experience. The lab experiments show that the method and calculations are correct. This can be seen as a proof of concept. The conclusions made of this thesis work is:

- The impedance of a shielded cable is proportional to the shield performance.

- A specific connector can be examined by measuring loop impedance and the voltage drop over the connector using a voltage probe.

- Programmable filters were made using switched capacitance filter ICs but it is important to amplify both before and after the filter to prevent too high attenuation.
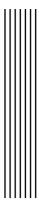
This prototype is far from perfect. The following improvements can be done to the measurement tool:

- The class-D amplifier should be changed to a class A amplifier to get a nice sine signal with constant frequency

- The measurement input signal should be amplified both before and after the filters to allow a high signal to noise ratio.

- The battery should have a better charging solution to allow the device to be turned off while charging.

- The DAC and ADCs should be replaced with external ICs since there is a risk that the connection between the two PCBs is affecting the measurement results.

- The development environment for the STM32 development board is very new and had a lot of problems. A better solution would be to use an older and less powerful MCU to simplify the software development.

Bibliography
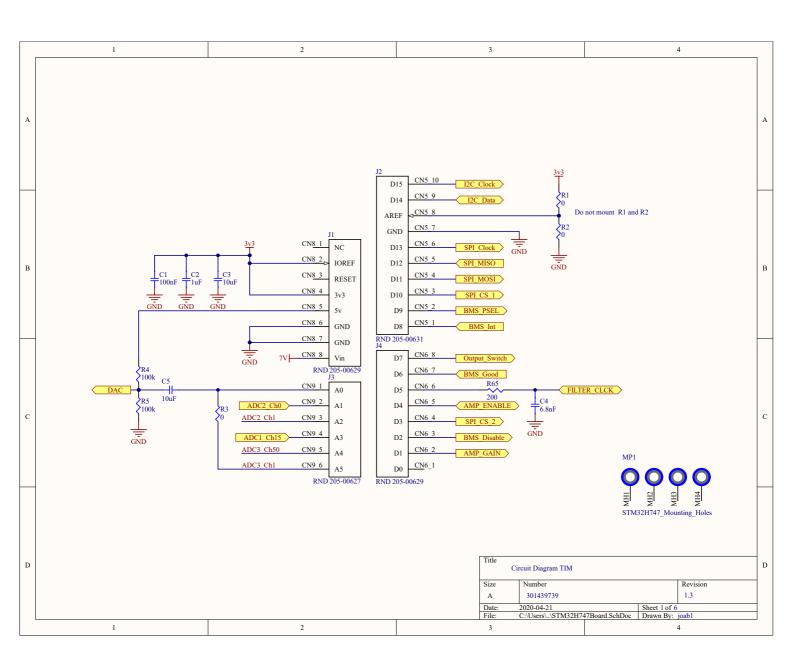
[1] Bogdan Adamczyk. *Current Probe Measurements in EMC Testing*. 2017. URL: https://incompliancemag.com/article/current-probe-measurements-in-emc-testing/.

[2] Biezl. *Stromwandler Zeichnung*. 2009. URL: https://commons.wikimedia.org/wiki/File:Stromwandler_Zeichnung.svg.

[3] Michel Mardiguian. "Simple Method for Predicting a Cable Shielding Factor, Based on Transfer Impedance". In: (2012).

[4] Michel Mardiguian. "Simple Method for Predicting a Cable Shielding Factor, Based on Transfer Impedance". In: *2012 EMC Directory & Design Guide* (2012).

[5] Ken Martin. "Improved circuits for the realization of switched-capacitor filters". In: *IEEE Transactions on Circuits and Systems* (1980).

[6] Abid Mushtaq and Stephan Frei. "Transfer impedance simulation and measurement methods to analyse shielding behaviour of HV cables used in Electric-Vehicles and Hybrid-Electric-Vehicles". In: *Advances in Radio Science* (2016).

[7] Radionics. *Solid State Relays: A Comprehensive Guide*. 2019. URL: https://ie.rs-online.com/web/generalDisplay.html?id=ideas-and-advice/solid-state-relays-guide.

[8] Sergei Alexander Schelkunoff. "The Electromagnetic Theory of Coaxial Transmission Lines and Cylindrical Shields". In: *The Bell System Technical Journal* 13.4 (1934), pp. 532–579.

[9] Amazon Web Services. *About RTOS*. 2020. URL: https://www.freertos.org/about-RTOS.html.

[10] ST. *UM2411 User Manual*. 2020. URL: https://www.st.com/resource/en/user_manual/dm00504240-discovery-kit-with-stm32h747xi-mcu-stmicroelectronics.pdf.

[11] R. Tiedemann and K.-H. Gonschorek. "Simple Method for the Determination of the Complex Cable Transfer Impedance". In: *1998 IEEE EMC Symposium. International Symposium on Electromagnetic Compatibility. Symposium Record* (1998).
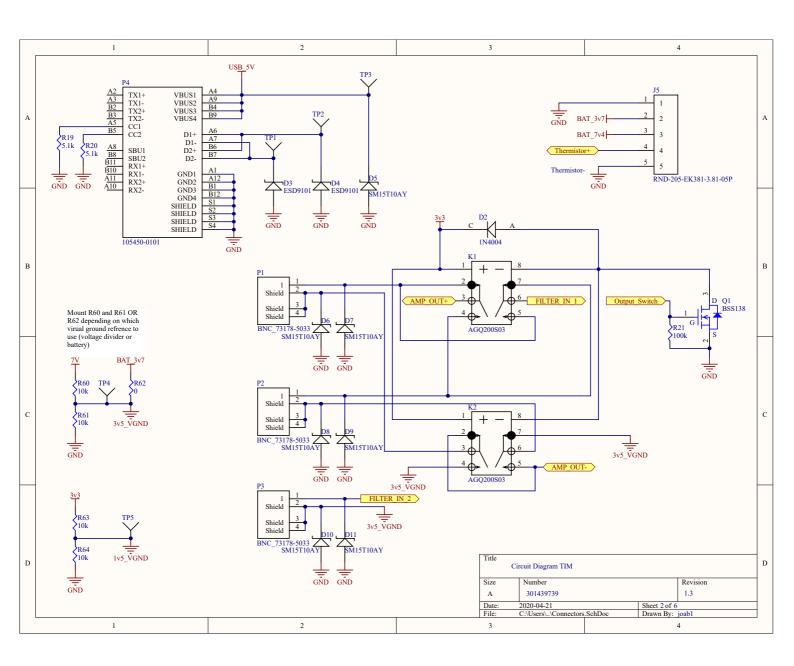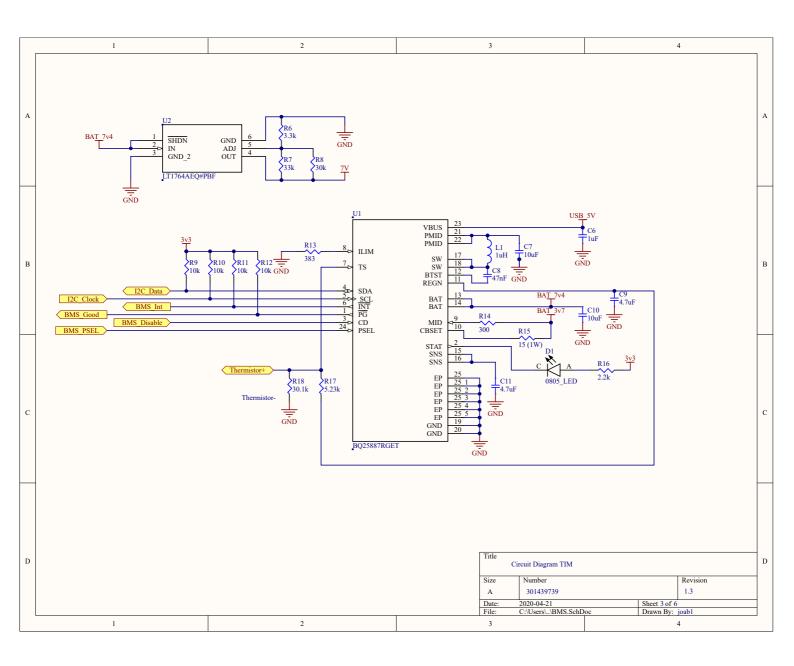
Appendices

A Circuit Diagram

Circuit Diagram TIM

Size	Number	Revision
A	301439739	1.3

Date: 2020-04-21 Sheet 2 of 6
File: C:\Users\..\Connectors.SchDoc Drawn By: joab1

Mount R60 and R61 OR R62 depending on which virual ground refrence to use (voltage divider or battery)

57

U2
BAT_7v4
1 SHDN
2 IN
3 GND_2
GND 6
ADJ 5
OUT 4
LT1764AEQ#PBF
GND

R6 3.3k
R7 33k
R8 30k
GND
7V

U1
3v3
R9 10k R10 10k R11 10k R12 10k GND
R13 383
8 ILIM
7 TS

I2C_Data
I2C_Clock
BMS_Int
BMS_Good
BMS_Disable
BMS_PSEL

4 SDA
5 SCL
6 INT
1 PG
3 CD
24 PSEL

Thermistor+
R18 30.1k R17 5.23k
Thermistor-
GND

VBUS 23
PMID 21
PMID 22
SW 17
SW 18
BTST 12
REGN 11
BAT 13
BAT 14
MID 9
CBSET 10
STAT 2
SNS 15
SNS 16
EP 25
EP 25_1
EP 25_2
EP 25_3
EP 25_4
EP 25_5
GND 19
GND 20

BQ25887RGET

USB_5V
C6 1uF
GND
L1 1uH
C7 10uF
GND
C8 47nF
GND

BAT_7v4
BAT_3v7
R14 300
R15 15 (1W)
C9 4.7uF
C10 10uF
GND
GND

D1
C A
0805_LED
R16 2.2k
3v3
C11 4.7uF
GND
GND

Title
Circuit Diagram TIM

Size A
Number 301439739
Revision 1.3
Date: 2020-04-21
File: C:\Users\..\BMS.SchDoc
Sheet 3 of 6
Drawn By: joab1

7V
C12 100uF
C13 0.1uF
C14 1nF
GND

7V
C15 100uF
C16 0.1uF
C17 1nF
GND

7V
C23 1uF
GND

U3

Pin	Name		Name	Pin
15	PVCCR	OUTPL	25
16	PVCCR	OUTNL	23
27	PVCCL	OUTNR	20
28	PVCCL	OUTPR	18
7	AVCC	BSPL	26
3	LINP	BSNL	22
4	LINN	BSNR	21
11	RINN	BSPR	17
12	RINP	GVDD	9
2	SD/FAULT		
5	GAIN_SEL		
6	MODE_SEL		
10	PLIMIT	GND	24
1	NC	GND	19
13	NC	GND	8
		AGND	14
		PAD	29

TPA3138D2

TP6
AMP_OUT+

TP7
AMP_OUT-

C18 0.47uF
C19 0.47uF

GND

C22 1uF
GND
C21 1uF

TP8
DAC

7V
R22 100k
R23 100k
R24 100k

3v3
TP19
R66 10k
G
TP20
S D
AMP_ENABLE
Q2 BSS138

3v3
TP21
R25 10k
G
TP22
S D
AMP_GAIN
Q3 BSS138

R27 0
R26 0
Don't mount R26
GND

C20 1uF
GND

Title			
Circuit Diagram TIM			
Size	Number		Revision
A	301439739		1.3
Date:	2020-04-21	Sheet 4 of 6	
File:	C:\Users\..\Amplifier.SchDoc	Drawn By: joab1	

B   Assembly Drawing

Document title:		
	PB Assembly Drawing TIM	
Date:	Issued by:	Document number:
2020-04-28	Johan Abrahamsson	301439738

C Drawing

Component Side (Scale: 1:1)

401028884

Drill Drawing View

108.00mm

127.00mm

5.08mm

5.08mm

Drill Table — Tolerance +/- 0.1 (mm)

Symbol	Count	Hole Size	Plated
A	8	0.90	Plated
B	143	0.40	Plated
C	5	1.30	Plated
D	6	2.00	Plated
E	32	0.80	Plated
F	4	3.50	Plated
G	25	0.60	Plated

Layer Structure

Layer	Thickness (um)
Text Print	No
Soldermask	Yes
Cu Layer 1	min 30 *
Laminate	
Cu Layer 2	35
Laminate	
Cu Layer 3	35
Laminate	
Cu Layer 4	min 30 *
Soldermask	Yes
Text Print	No

* incl plating

1.6 +/- 0.16

65

UNLESS OTHERWISE SPECIFIED:
DIMENSIONS ARE IN MILLIMETERS
SURFACE FINISH:
TOLERANCES:

FINISH:

DEBURR AND BREAK SHARP EDGES

DO NOT SCALE DRAWING

REVISION

	NAME	SIGNATURE	DATA
DRAW	joab1		
CHKD			
APPVD			
MFG			
QA			

MATERIAL:

WEIGHT:

TITLE:

PB Drawing TIM

DWG N0.

301439741

SCALE 1:1

A0